Res Chem Intermed
https://doi.org/10.1007/s11164-018-3388-y

Production of activated carbon as catalyst support by microwave pyrolysis of palm kernel shell: a comparative study of chemical versus physical activation

Rock Keey Liew[1] · Min Yee Chong[1] · Osarieme Uyi Osazuwa[2] · Wai Lun Nam[1] · Xue Yee Phang[1] · Man Huan Su[1] · Chin Kui Cheng[2] · Cheng Tung Chong[3] · Su Shiung Lam[1]

Received: 20 July 2017 / Accepted: 12 September 2017

Abstract Palm kernel shell (PKS), representing an abundantly available oil palm waste in Malaysia, was transformed into activated carbon by microwave vacuum pyrolysis. PKS was first carbonized to produce biochar, followed by an activation process with chemical or water to produce chemically and physically activated carbon, respectively. The activated carbon materials were characterized for their porous characteristics and elemental and proximate composition to examine their suitability as catalyst support. Catalysts were synthesized by supporting nickel on the activated carbon materials and

✉ Su Shiung Lam
lam@umt.edu.my; sushiung@gmail.com

Rock Keey Liew
lrklrk1991@gmail.com

Min Yee Chong
min5201@hotmail.com

Osarieme Uyi Osazuwa
osarieme.osazuwa@uniben.edu

Wai Lun Nam
lunnw0301@gmail.com

Xue Yee Phang
p.xue.yee@hotmail.com

Man Huan Su
manhuan93@gmail.com

Chin Kui Cheng
chinkui@ump.edu.my

Cheng Tung Chong
ctchong@mail.fkm.utm.my

[1] Pyrolysis Technology Research Group, Eastern Corridor Renewable Energy Group (ECRE), School of Ocean Engineering, Universiti Malaysia Terengganu, 21030 Kuala Nerus, Terengganu, Malaysia

Published online: 14 March 2018

tested for their performance in the methane dry reforming reaction. Microwave vacuum pyrolysis of PKS-derived char resulted in up to 89 wt% yield of activated carbon. The activated carbon was detected to have high Brunauer–Emmett–Teller (BET) surface area associated with a highly porous surface, characteristics of high adsorption capacity corresponding to many sites for adsorption of metal atoms with great potential for use as catalyst support material. Nickel atoms were detected on the surface of the activated carbon catalyst support, indicating successful synthesis of nickel-supported catalyst. The catalysts showed high methane conversion (up to 43 %), producing approximately 22 % gaseous products ($CO + H_2$). These results show that activated carbon produced from microwave pyrolysis of palm kernel shell is a promising catalyst support material. Chemically activated carbon performed better as catalyst support compared with physically activated carbon in terms of CH_4 and CO_2 conversions.

Graphical Abstract

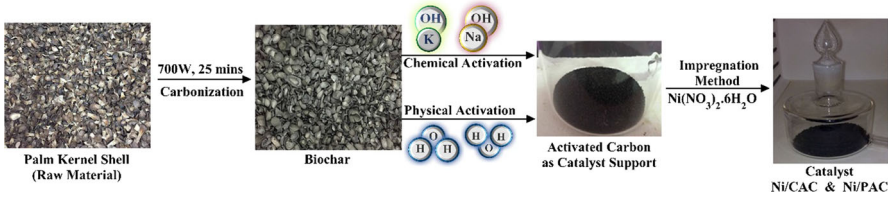

Keywords Palm · Activated carbon · Pyrolysis · Microwave · Catalyst support

Introduction

Catalysts promote the rate of chemical reactions by lowering the activation energy between reactants and products [1]. There are two types of catalyst, namely unsupported (or bulk) and supported. An unsupported catalyst comprises only active material such as metals, metal oxides, carbides, and nitrides, whereas a supported catalyst consists of small amounts of active material impregnated on the surface of a supporting material termed the catalyst support (e.g., SiO_2, TiO_2, and alumina) [2]. Catalysts play a significant role in controlling the efficiency of industrial processes; For example, catalyst use is essential in Fischer–Tropsch synthesis to speed up the reaction rate and increase the productivity of liquid fuel from biomass [3]. For applications in industry and research, supported catalysts are deemed to be more applicable than unsupported catalysts for several reasons, such as high tolerance to sulfur poisoning [4, 5], ability to be reused multiple times without significant degradation [6], and higher catalytic activity in certain chemical reactions (e.g.,

[2] Faculty of Chemical and Natural Resources Engineering, Universiti Malaysia Pahang, Lebuhraya Tun Razak, 26300 Gambang, Kuantan, Pahang, Malaysia

[3] Faculty of Mechanical Engineering, Universiti Teknologi Malaysia, 81310 Skudai, Johor, Malaysia

Suzuki–Miyaura cross-coupling reaction) [6]. However, the market price of conventional catalyst supports is high due to their manufacturing cost [4]. Hence, further efforts should be made to identify cheaper materials as alternatives to commercial catalyst support materials.

Recently, there has been increasing interest in recovery of carbon-based materials (e.g. carbon nanotubes, and granular and powdered carbon) from waste and biomass materials for use as catalysts or catalyst supports [7–10]. Some such materials (e.g., carbon nanotubes and mesoporous carbon) show promising properties such as good thermal stability and have been utilized recently as catalyst supports for catalytic applications in fuel cells, sensors, and solar cells [11, 12]. In contrast, there have been only limited studies on production of activated carbon from waste materials for use as catalyst support. Existing literature is limited to studies performed recently by Meryemoglu et al. [13] on application of activated carbon derived from kenaf biomass as catalyst support in an aqueous-phase reforming process, and a more recent examination by Dhelipan et al. [14] on utilization of orange peel activated carbon as catalyst support for the oxygen reduction reaction in proton exchange membrane fuel cells.

Activated carbon is an amorphous carbonaceous material with high surface porosity and large surface area ($\geq$800 m^2/g) [15]. Activated carbon also possesses relatively high chemical inertness, which can avoid unnecessary chemical reactions with the reactant, thus representing a chemically stable material for use as a catalyst support in heterogeneous catalytic reactions [16]. It was thought that application of activated carbon as catalyst support could be a cheaper alternative to substitute for expensive conventional catalyst supports (e.g., alumina and SiO_2), since activated carbon is produced from waste and biomass materials that are either low cost or free of charge.

Two approaches are used to produce activated carbon, namely one- and two-step methods. Using the one-step approach, the feedstock can be directly transformed into activated carbon via simultaneous carbonization and activation reactions. In the two-step approach, the feedstock needs to undergo carbonization (to produce char) as a first step followed by activation as a second step to form activated carbon. It has been reported that the two-step approach is preferred as activated carbon with higher surface area is obtained compared with when using the one-step approach [17]. To perform the two-step approach, the feedstock is first carbonized to produce a carbon-dense biochar by pyrolysis (i.e., a thermal decomposition process under inert environment) [18–22], then subjected to either physical or chemical activation to produce activated carbon [23]. For physical activation, steam or carbon dioxide is used as activating agent in the activation process, whereas chemicals such as potassium hydroxide, sodium hydroxide, or zinc chloride are utilized as dehydrating agents in chemical activation.

Physical activation produces activated carbon with different pore sizes depending on the type of activating agent used (i.e., carbon dioxide, steam, or mixture therefore); For instance, use of carbon dioxide produces activated carbon with mainly micropores, whereas steam can increase the pore size and produce mesoporous activated carbon [23]. During physical activation, the remaining volatile materials and tar present in the biochar are decomposed via gasification

($C + H_2O \rightarrow CO + H_2$) [24] or Boudouard reaction ($C + CO_2 \rightarrow 2CO$) [25]. Production and emission of gases such as CO and H_2 from the biochar surface then either results in new pores or widens existing pores, producing activated carbon with high porosity [26].

In chemical activation, use of chemicals (e.g. KOH, NaOH, and $ZnCl_2$) either weakens or breaks chemical bonds between the lignocellulosic content remaining in the biochar, transforming it to smaller organic fractions such as CO_2 and CH_4 that are removed during subsequent thermal treatment by pyrolysis, resulting in formation of activated carbon with well-developed porous structure [27]. It has been reported that alkali chemical agents (e.g., KOH) result in activated carbon with high micropore volume and narrow pore size, whereas acidic chemical agents (e.g., H_3PO_4) yield high macropore volume and broader pore size distribution [28].

The findings above provide the motivation for this study. We conducted experiments to produce activated carbon from palm kernel shell using both chemical and physical activation with the aim of assessing its potential for use as catalyst support. Palm kernel shell (PKS), representing an abundantly available oil palm waste in Malaysia, was transformed into activated carbon using a two-step approach. The activated carbon obtained was extensively characterized in terms of its surface characteristics and elemental and proximate compositions. The activated carbon was then synthesized into a supported nickel catalyst and applied in the methane dry reforming process to evaluate the feasibility of using such PKS-activated carbon (AC) as catalyst support material.

Materials and methods

Chemicals used in preparation of AC and synthesis of catalyst

Potassium hydroxide (KOH) and sodium hydroxide pellets (QREC) with purity $\geq$85 % were used as the chemical activating agent to prepare chemically activated carbon. Nickel nitrate hexahydrate [$Ni(NO_3)_2 \cdot 6H_2O$] (Sigma-Aldrich) with purity of 99.99% was used in catalyst synthesis. After chemical activation, 12 M hydrochloric acid (QREC) was used in a washing step to remove residual chemical. Concentrated sulfuric acid (QREC) was used in determination of lignin content.

Pretreatment of palm kernel shell

Palm kernel shell (PKS) was collected from the oil palm mill owned by TDM Plantation Sdn Bhd., located in Kemaman, Terengganu, Malaysia. PKS was washed with tap water to remove dirt and dried in an oven for 24 h at 110 °C to eliminate moisture content to prevent rotting [29]. The dried shells were ground into small pieces (<5 mm) using a grinder and stored in a closed container for future use.

Characterization of palm kernel shell

Elemental analysis was conducted using a CHNS elemental analyzer to quantify the elemental content of carbon, hydrogen, nitrogen, and sulfur present in PKS; the oxygen content was obtained by the mass difference (i.e., O = 100−C−H−N−S) [19]. PKS was also analyzed by thermogravimetric analysis (TGA) under N_2 environment to determine the contents of moisture and volatile matter. The ash content was quantified by combustion of the sample in a furnace at 950 °C with holding time of 10 min, whereas the fixed carbon was calculated by mass difference (i.e., fixed carbon = 100 − moisture − volatile matter − ash) [15]. The method for lignin content determination was adapted and modified from Carrier et al. [30], based on soaking PKS in 72 % sulfuric acid (H_2SO_4) at room temperature for 2 h followed by reflux at 100 °C for 2 h. The mixture was filtered, and the residue obtained was washed with distilled water to pH 7.0. The residue was dried in an oven, and finally the content of lignin (wt%) was obtained. For determination of the cellulose content of PKS, it was soaked in 17.5 % concentration NaOH at room temperature for 30 min. The resulting mixture was filtered, and the residue was washed with distilled water to neutral pH, followed by impregnation with 10 % concentration acetic acid for 1 h. The mixture was filtered and washed with hot water to neutral pH. The residue was then dried in an oven to obtain the content of cellulose (wt%) [30]. The content of hemicellulose was estimated by mass difference (i.e., hemicellulose = 100 wt% − lignin − cellulose).

Preparation of activated carbon (AC) via microwave vacuum pyrolysis of palm kernel shell

Carbonization of palm kernel shell to produce biochar

A two-step approach was applied to prepare activated carbon, in which the palm kernel was first subjected to carbonization followed by activation using chemical or water. A modified commercial microwave oven operating at frequency of 2.45 GHz was used, and connected to a temperature logger to monitor the temperature throughout the experiment. Before carbonization was initiated, the air inside the microwave oven cavity was removed using a vacuum pump connected to the microwave oven to create an inert environment for the carbonization reaction to occur [31, 32]. Approximately 100 g PKS was weighed then carbonized in the microwave oven at 700 W for 25 min. It was ascertained in a trial experiment that no emission of pyrolysis volatiles was observed after 20 min of pyrolysis of PKS, thus microwave irradiation time of 25 min was chosen to allow the pyrolysis process to complete [31]. An approximately 40 wt% yield of biochar was collected, sieved to 0.1 mm, and further subjected to activation for conversion to activated carbon.

Microwave pyrolysis with chemical activation using hydroxide mixture

The procedure for chemical activation was adapted from Lam et al. [15]. A hydroxide mixture solution was first prepared by dissolving potassium and sodium

hydroxide at weight ratio of 1:1 in distilled water. Then, biochar was immersed in the prepared solution, which was stirred and heated using hot plate until the mixture boiled to form a slurry. Heating was stopped, and the slurry was left for 24 h. The slurry was filtered to obtain biochar impregnated with hydroxides, which was then subjected to microwave pyrolysis (700 W, 25 min) for conversion to AC. The resulting AC was washed thoroughly using 0.1 M HCl to neutralize the pH to around 7.0 followed by rinsing with hot water to remove residual chemical (e.g., KCl and NaCl) in the AC. The AC obtained (termed "CAC") was dried in an oven at 110 °C for 24 h. The dried CAC was characterized and subsequently synthesized into a catalyst to assess its potential as a catalyst support.

Microwave pyrolysis with physical activation using water

Biochar produced as described above was first immersed in water and boiled for 10 min, then transferred to a reactor; water was added at reaction ratio of 1:10, defined as the weight of biochar (in g) to the volume of water (in ml). The biochar was activated using water in the microwave oven at microwave power of 700 W for 25 min. After 25 min, a certain volume of water was added again to the resulted product, and activation was performed a second time using microwave pyrolysis. The AC obtained was cooled to room temperature and stored in a sample vial. The AC was then characterized and subsequently synthesized into a catalyst to assess its potential as a catalyst support. The final product is termed "PAC."

Characterization of CAC and PAC

The elemental (C, H, N, S, O) and proximate contents (moisture, volatile matter, fixed carbon, and ash) of the samples were obtained according to the aforementioned method. The porous characteristics of the samples were analyzed using a surface porosimeter to estimate pore size, pore volume, and surface area. The surface area was estimated using the multipoint Brunauer–Emmett–Teller (BET) method, whereas the total pore volume and pore size were estimated using the Barrett–Joyner–Halenda (BJH) method. The pore size distribution of the samples was estimated using a density functional theory (DFT) model [33]. The surface morphology of the samples was also examined using scanning electron microscopy (SEM) at accelerating voltage of 15 kV and magnification of 1000×.

Synthesis and characterization of nickel catalyst supported on CAC and PAC

The catalyst was synthesized using the method adapted from Lam et al. [5]. Nickel nitrate solution with concentration of 0.58 M was prepared by dissolving 2.63 g nickel nitrate in distilled water. The resulting solution was heated from ambient temperature to 80 °C. AC (10 g) was weighed and mixed with nickel nitrate solution. The mixture was heated and maintained at 80 °C with continuous stirring for 1 h. The mixture was then dried in an oven at 110 °C for 24 h. Next, the dried product was calcined in a furnace under inert environment from ambient

temperature to 300 °C at heating rate of 10 °C/min for 1 h [9]. The catalysts produced are termed "Ni/CAC" and "Ni/PAC." The catalysts produced were quantified for their element composition using energy-dispersive X-ray spectroscopy (EDX) at accelerating voltage of 20 kV. The porous characteristics (surface area, porous volume, and pore size) of the catalysts were also evaluated by surface porosimeter.

Application of Ni/CAC and Ni/PAC

Catalytic testing was performed in a stainless-steel fixed-bed reactor. The reactor was loaded with 0.1 g catalyst supported on quartz wool and placed in a tube furnace. The catalyst was reduced using 50 vol% H_2/N_2 at flow rate of 50 ml/min over a range of process times (0.25–2.0 h) at 1073 K. Subsequently, the reactant gas mixture (CO_2 and CH_4) was purged with nitrogen as carrier gas at flow rate of 50 ml/min and gas hourly space velocity of 30,000 mL h^{-1} g^{-1} over the reduced catalyst. The composition of the outlet gas, consisting of reactants (CO_2 and CH_4) and products (H_2 and CO), was analyzed by gas chromatography–thermal conductivity detector (GC-TCD). Helium (20 ml/min) was used as carrier gas at column operating temperature of 393 K. The conversions of the reactant gases (i.e., CH_4 and CO_2) and the yields of H_2 and CO were calculated using Eqs. 1–4 [34, 35].

$$\text{Conversion of } CO_2 = \left[\frac{\text{flow rate of } CO_2(\text{in}) - \text{flow rate of } CO_2(\text{out})}{\text{flow rate of } CO_2(\text{in})} \times 100\,\%\right], \tag{1}$$

$$\text{Conversion of } CH_4 = \left[\frac{\text{flow rate of } CH_4(\text{in}) - \text{flow rate of } CH_4(\text{out})}{\text{flow rate of } CH_4(\text{in})} \times 100\,\%\right], \tag{2}$$

$$\text{Yield of } H_2 = \left[\frac{\text{flow rate of } H_2(\text{out})}{2 \times \text{flow rate of } CH_4(\text{in})} \times 100\,\%\right], \tag{3}$$

$$\text{Yield of CO} = \left[\frac{\text{flow rate of CO (out)}}{\text{flow rate of } CH_4(\text{in}) + \text{flow rate of } CO_2(\text{in})} \times 100\,\%\right]. \tag{4}$$

Results and discussion

Characterization of palm kernel shell (PKS)

Table 1 presents the lignocellulosic and chemical contents of PKS obtained from elemental and proximate analyses. PKS showed high content of lignin (48 wt%), followed by cellulose (30 wt%) and hemicellulose (22 wt%). The majority of PKS was carbon (51 wt%) and oxygen (39 wt%) with low content of hydrogen and nitrogen of 3 and 7 wt%, respectively. In addition, PKS was dominated by volatile

Table 1 Lignocellulosic, elemental, and proximate contents (wt%) of PKS

	PKS
Lignocellulosic content[a]	
Cellulose	30
Hemicellulose[b]	22
Lignin	48
Elemental content[c]	
Carbon	51
Hydrogen	3
Nitrogen	7
Oxygen[d]	39
Sulfur[e]	0
Proximate content[f]	
Moisture	4
Volatile matter	53
Fixed carbon[g]	40
Ash[h]	3

[a]Dry basis

[b]Estimated by difference (i.e., hemicellulose = 100 wt% − cellulose − lignin)

[c]Dry ash-free basis

[d]Calculated by mass difference (i.e., oxygen = 100 wt% − C − H − N − S)

[e]Not detectable due to the minimum detection limit of the CHNS analyzer (<0.05 wt%), thus assumed to be 0 wt% in calculation

[f]Dry basis

[g]Calculated by mass difference (i.e., fixed carbon = 100 wt% − moisture − volatile matter − ash)

[h]Obtained by combustion at 950 °C with holding time of 10 min

matter (53 wt%) and fixed carbon (40 wt%) with small amounts of moisture (4 wt%) and ash (3 wt%).

PKS showed almost 50 wt% lignin content, being comparatively the highest compared with other oil palm waste materials (i.e., empty fruit bunch, mesocarp fiber, oil palm trunk, and frond) with 21–35 wt% lignin content [36–39]. Thus, higher yield of carbon-dense material such as biochar could be recovered from PKS due to the complex polymeric structure of lignin [40]. Most of the benzene rings that are abundantly present within the lignin structure possess higher chemical stability against decomposition reaction compared with the polysaccharide units present in cellulose and hemicellulose. Consequently, lignin will be transformed and rearranged into a more stable form of biochar with higher aromaticity during the carbonization process [41], rather than being decomposed into smaller organic compounds to form condensable bio-oil or incondensable gases such as CH_4, CO_2, and CO via depolymerization and fragmentation [42].

In addition, high contents of carbon and fixed carbon were detected in PKS, indicating its suitability for conversion into carbon-dense materials such as biochar and activated carbon using the pyrolysis process. However, PKS also contained high

amounts of oxygen and volatile matter, suggesting that these contents should be removed to produce a carbon-dense product, otherwise these oxygenated volatiles could react with reactants or products to produce byproducts (e.g. oxidized reactants and products) during the catalytic reactions. Alternatively, these oxygenated volatiles could be recovered and used as potential fuel or chemical feedstock [43–46].

Microwave vacuum pyrolysis conversion of PKS to AC

Product yield and proximate and elemental compositions (wt%) of AC

Table 2 presents the yield and proximate and elemental compositions of the AC materials, revealing up to 89 wt% yield when using the microwave vacuum pyrolysis approach. Fixed carbon (81–85 wt%) represents the main content detected in AC, followed by volatile matter (6–10 wt%) and small amounts of moisture (4–6 wt%) and ash (3–5 wt%). The AC was also dominated by both carbon (70–78 wt%) and oxygen (17–27 wt%), whereas nitrogen (1 wt%) and hydrogen (2–4 wt%) were detected in low amounts.

Table 2 Product yield and proximate and elemental compositions of AC

	CAC[h]	PAC[i]
Proximate content[a]		
Moisture	4	6
Volatile matter	6	10
Fixed carbon[b]	85	81
Ash[c]	5	3
Elemental content[d]		
Carbon	78	70
Nitrogen	1	1
Hydrogen	4	2
Oxygen[e]	17	27
Sulfur[f]	0	0
Product yield[g]	89	84

[a]Dry basis

[b]Calculated by difference (fixed carbon = 100 wt% − moisture − volatile matter − ash)

[c]Obtained by combustion in furnace at 950 °C for 10 min

[d]Dry ash-free basis

[e]Calculated by mass difference (i.e., oxygen = 100 wt% − C − H − N − S)

[f]Not detectable due to the minimum detection limit of the CHNS analyzer (<0.05 wt%) thus assumed to be 0 wt% in calculation

[g]Yield of AC = [dried mass of AC produced/dried mass of biochar used] × 100 %

[h]Activated carbon produced by chemical activation

[i]Activated carbon produced by physical activation

It was found that the yield of CAC was slightly higher than PAC, which can be attributed to the different mechanism of the chemical reactions occurring. During chemical activation, hydroxyl ions (OH^-) are likely to have broken chemical bonds between the lignocellulosic components remaining in the biochar, leading to their removal in the form of volatiles (e.g., CH_4 and H_2) during the subsequent thermal treatment [15], leaving the nonvolatile fraction as the final yield of the CAC. In contrast, the water reacted differently with the biochar during physical activation. When microwave heating was applied to the mixture of biochar and water, water molecules (H_2O) reacted directly with carbon (C) atoms present in the biochar, resulting in production of carbon monoxide (CO) and hydrogen (H_2) as gaseous products. In addition, water activation was done twice, indicating that more carbon atoms were transformed into gaseous form when the overall activation process was completed. This explains the lower yield of PAC compared with CAC.

Both the fixed carbon and carbon contents of the CAC and PAC increased significantly after the activation process, whereas the volatile matter and oxygen contents decreased dramatically. This can be attributed to further decomposition reactions that happened during the activation process. The remaining lignocellulosic contents (e.g., cellulose, hemicellulose, and lignin) present within the biochar were either depolymerized into smaller units such as furfural and levomannosan [42] or fragmented into light organic molecules (e.g., CO_2 and CH_4) and released in the form of volatiles. As a result, CAC and PAC were concentrated in terms of carbon content after removal of these oxygenated volatiles. Carbon-rich AC can show high chemical resistance and therefore low reactivity in reactions such as hydrolysis, and acid and base reactions. Hence, it is envisaged that both AC materials could be used as support for catalysts for such reactions. Low reactivity could also improve the durability of the catalyst supports. The ash content of both AC materials produced was detected to lie within the commercially acceptable range ($\leq$5 wt%); higher ash content (>5 wt%) could occupy available adsorption sites, thus decreasing the adsorption capacity for metal atoms, making the AC undesirable for use as catalyst support.

Figure 1 depicts the proposed reaction mechanism for formation of PAC and CAC via microwave vacuum pyrolysis of PKS. During biochar formation, the lignocellulosic contents (i.e., lignin, cellulose, and hemicellulose) present in PKS likely underwent several reactions such as rupture of alkyl–aryl linkages present within the lignin component, depolymerization, fragmentation, and dehydration of cellulose and hemicellulose contents [42], hence producing a biochar matrix that could contain polyaromatic structure with polymer units of cellulose and hemicellulose. The biochar matrix was activated either chemically using alkali-metal hydroxides (i.e., NaOH and KOH) or physically using water, to form CAC and PAC, respectively.

During chemical activation, hydroxyl ions (OH^-) likely attacked the chemical bonds between the polymer units of cellulose and hemicellulose remaining within the biochar matrix, resulting in their decomposition in the form of volatiles (e.g., CH_4 and CO_2) during the subsequent thermal treatment [15]. Meanwhile, the polyaromatic structure derived from lignin could undergo rearrangement reaction [42], during which the polyaromatic structure would be combined to form a more

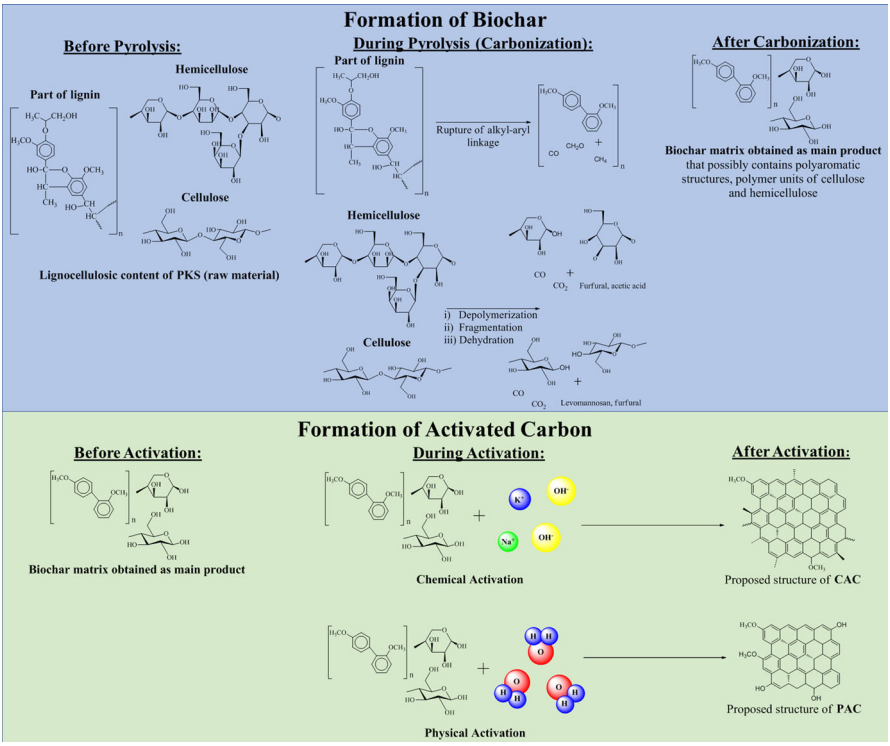

Fig. 1 Proposed reaction mechanism for formation of PAC and CAC

complex carbon structure (i.e., CAC) having higher aromaticity. During physical activation, water molecules were likely to react with the biochar matrix when microwave heating was applied. Water molecules (H_2O) could react directly with carbon (C) atoms present in the biochar matrix, resulting in production of carbon monoxide (CO) and hydrogen (H_2) as gaseous products, thus producing PAC with lower carbon content (70 wt%; Table 2).

Surface morphology of AC

Figure 2a and b show SEM micrographs of PAC and CAC. Many pores were observed on the surface of the AC obtained, indicating that the decomposition reactions occurring during activation led to production and release of the remaining volatile matter from the biochar, thus the remaining nonvolatile components were transformed into AC with pores of different shapes and sizes as observed on the surface. The presence of these porous structures further supports the potential use of AC as catalyst support, since such pores could provide sites on which catalytically active materials (e.g. metal atoms and metal oxides) could be adsorbed to form an active catalyst [47].

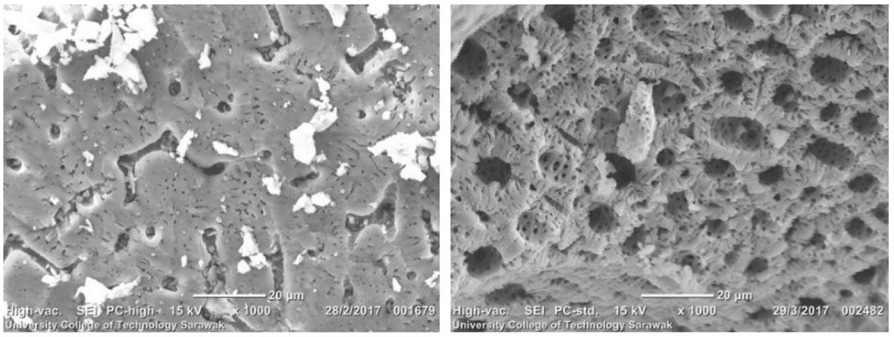

(a) **(b)**

Fig. 2 SEM image of **a** PAC and **b** CAC

It was also observed that AC with different pore sizes, shapes, and distribution was obtained using the different activation methods. PAC (Fig. 2a) contained pores with irregular shape and size. In contrast, the majority of the pores found on the surface of CAC (Fig. 2b) showed circular shape with a pattern of small pores contained in the inner layer of large pores. This can be explained by the intercalation effect caused by the interaction of the alkali-metal atoms (i.e., K and Na) with the carbon structure of AC [44, 48]. K and Na atoms would react differently with the carbon structure during thermal treatment and penetrate into the inner layer of the activated carbon, resulting in the formation of smaller pores within the larger pores after the subsequent washing step.

Porous characteristics of AC

Table 3 presents the porous characteristics of the AC obtained. The AC was found to exhibit high BET surface area ranging from 480 to 750 m^2/g. Release of volatiles from the biochar on pyrolysis likely led to creation of pores (or void spaces) in the remaining nonvolatile fraction (i.e., carbon) within the biochar, which was in turn transformed into activated carbon. The average pore size of the activated carbon materials (4.4–4.8 nm) lay within the range of 2–50 nm, indicating that the

Table 3 Porous characteristics of AC

Property	PAC[a]	CAC[b]
BET surface area (m^2/g)[c]	480	750
Total pore volume (cm^3/g)[d]	0.26	0.37
Average pore size (nm)[d]	4.4	4.8

[a]Activated carbon produced by physical activation

[b]Activated carbon produced by chemical activation

[c]Multipoint Brunauer–Emmett–Teller (BET) method

[d]Barrett–Joyner–Halenda (BJH) method

activated carbon produced was mesoporous according to the International Union of Pure and Applied Chemistry (IUPAC) classification [49]. Figure 3 shows the DFT pore size distribution for CAC and PAC, revealing that CAC exhibited a broader pore size distribution than PAC, which further corroborates the higher total pore volume (0.37 cm^3/g) obtained for CAC. In addition, the broader pore size distribution of CAC is supported by its surface morphology (Fig. 2b) in which pores with smaller sizes were contained in the inner layer of large pores. In contrast, the narrower pore size distribution of PAC also corroborates its surface morphology (Fig. 2a), where pores were observed on the surface while inner pores were barely seen, indicating that fewer inner pores were formed in PAC and hence lower total pore volume (0.26 cm^3/g) was obtained. These results suggest that AC with broader pore size distribution could be produced using chemical activation.

Furthermore, CAC showed higher BET surface area and total pore volume than PAC, which can be explained based on the use of alkali-metal hydroxides that acted as a dehydrating agent during the activation process to produce CAC [50]. Due to this dehydrating effect, the impregnated biochar could have undergone various chemical reactions (e.g., dehydration and decarboxylation) after the subsequent thermal treatment with release of volatile organic compounds. Emission of these volatile contents then formed void spaces (or pores) on the surface of the resulting activated carbon. Overall, these highly porous activated carbon materials (PAC and CAC) show promise for use as catalyst support material.

Properties of catalysts synthesized using activated carbons and their performance in catalytic application

Both activated carbons (PAC and CAC) were used as catalyst support for synthesis of supported nickel catalysts (i.e., Ni/PAC and Ni/CAC) via an impregnation method [47]. The Ni/PAC and Ni/CAC catalysts showed lower BET surface area (456–682 m^2/g) and pore volume (0.22–0.30 cm^3/g) than their respective AC, suggesting that impregnation of nickel atoms on the AC surface blocked some of the pores, thus decreasing the accessible surface area and pore volume located inside the pores. In addition to the lower BET surface area and pore volume of the

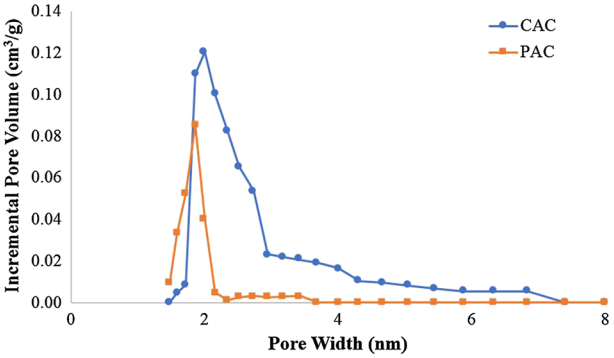

Fig. 3 DFT pore size distributions for PAC and CAC

catalysts, it is likely that the nickel nitrate hexahydrate (source of nickel atoms) that initially impregnated the surface of the AC decomposed and released its nitrate (NO_3^-) ligand and hydration shell (H_2O) during the calcination process. These nitrates and water molecules could further react with the carbon structure present within the AC and destroy some of the internal carbon structure of AC, resulting in production of catalysts with lower surface area and pore volume. SEM–EDX analysis was performed on the catalysts to confirm presence of nickel atoms on the surface of AC. Approximately 19 and 19.3 wt% nickel element was detected (at 7.471 keV) on the surface of Ni/PAC and Ni/CAC, respectively, providing evidence of successful impregnation of nickel atoms on the surface of AC.

The catalysts were tested in the methane dry reforming reaction to evaluate their performance in the conversion of the reactant gases (i.e., CO_2 and CH_4) into the gaseous products (H_2 and CO). Figure 4 shows the results obtained from the application of Ni/PAC and Ni/CAC in the catalytic reaction over a range of process times (0.25–2.0 h). The catalytic activity of the bare carbon supports (i.e., CAC and PAC) was also tested to investigate whether the methane dry reforming reaction would occur without loading the active material (Ni). However, neither CAC nor PAC showed any catalytic activity, hence these data are not included in Fig. 4. Up to 43 % of CH_4 plus 31 % of CO_2 were converted into 11–16 % of CO and small amounts of H_2 (3–6 %).

Equations 5–8 show the possible reaction mechanism occurring during the methane dry reforming process. Equation 5 represents the rate-determining step, in

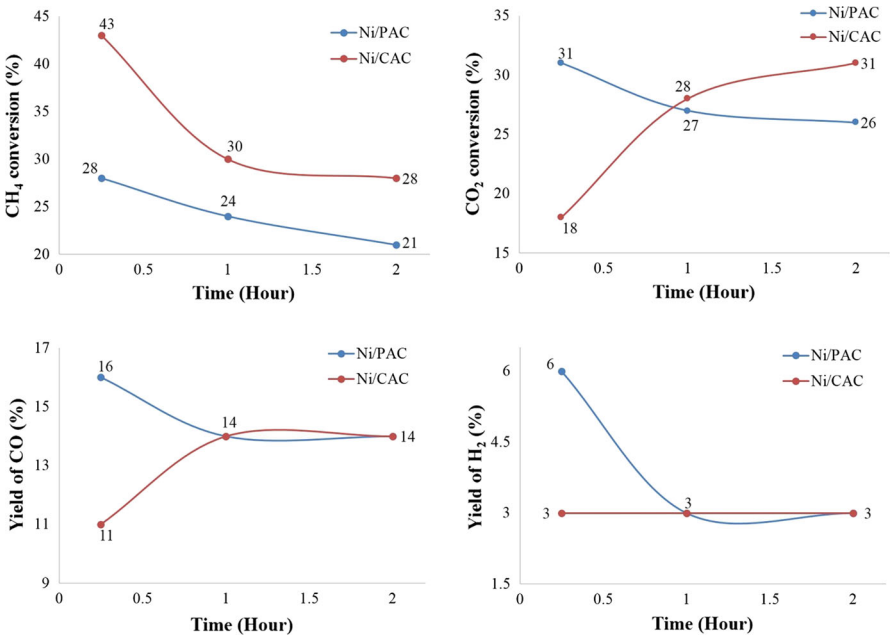

Fig. 4 Performance of Ni/PAC and Ni/CAC in methane dry reforming reaction. Zero catalytic activity was obtained for CAC and PAC, hence these data are not included in the graphs

which methane (CH_4) can dissociate into methylene species (CH_2) and hydrogen (H_2) on an active site of the catalyst [51]. Then, carbon dioxide (CO_2) can dissociate into CO and an intermediate oxygen species, and this oxygen species could then react with H_2 to form water via the reverse water–gas shift reaction. Finally, the water molecule can then react with CH_2 to yield CO and H_2 [52].

$$CH_4 \rightarrow CH_2 + H_2 \tag{5}$$

$$CO_2 \rightarrow CO + O \tag{6}$$

$$O + H_2 \rightarrow H_2O \tag{7}$$

$$H_2O + CH_2 \rightarrow CO + 2H_2 \tag{8}$$

It was found that the conversion efficiency of methane (CH_4) was decreased when the process time was increased from 0.25 to 2 h, indicating that the conversion of methane should be performed in shorter process time to obtain higher conversion efficiency. The lower conversion efficiency of methane recorded at longer process time could be due to coke formation on the catalyst surface, which would decrease methane conversion. It was expected that the Ni/PAC catalyst would show higher conversion efficiency of methane due to its higher oxygen content (27 wt%) on the AC surface, since oxygen will react with CH_4 to form O–CH_4, subsequently producing H_2 [35]. This concurs with the hydrogen yield results, in which Ni/PAC produced more hydrogen than Ni/CAC. However, Ni/CAC converted more methane than Ni/PAC throughout the overall process time, representing a great conflict in the results. This phenomenon can be attributed to the higher BET surface area (682 m^2/g) and pore volume (0.30 cm^3/g) of Ni/CAC, resulting in more reaction sites for methane conversion to occur. However, further studies are required to justify this phenomenon.

Ni/CAC showed an increasing trend of CO_2 conversion rate (from 18 to 31 %) as the process time was increased, but Ni/PAC recorded an opposite trend (from 31 to 26 %). This corroborates with the CO yield recorded for both catalysts, where increasing yield was obtained from Ni/CAC at longer process time. This indicates that the catalyst prepared from the chemically activated carbon showed lower conversion rate of CO_2 since longer process time was needed to convert CO_2 to CO. In contrast, the catalyst supported on physically activated carbon (Ni/PAC) is more suitable for CO_2 conversion in shorter process time to produce more CO. Further investigation of the chemical interactions in the described process are required to fully understand the reaction mechanism, due to the unusual results and significant difference between those obtained for Ni/CAC and Ni/PAC.

Conclusions

Palm kernel shell (PKS) showed high lignin (48 wt%), carbon (51 wt%), and fixed carbon (40 wt%) contents, thus showing potential for conversion into carbon-dense material such as biochar and activated carbon by pyrolysis. Around 40 wt% yield of

biochar was achieved by microwave vacuum pyrolysis of PKS for activation and conversion into CAC and PAC, respectively. Both AC materials showed high fixed carbon content with low volatile matter, indicating high resistance towards chemical reactions and thus being considered to be chemically stable. The AC materials were also found to have highly porous structure with high surface area (up to 750 m^2/g) and pore volume (up to 0.37 cm^3/g), suggesting suitability for use as catalyst support, since this can provide many reaction sites for metal atom impregnation. The AC materials were upgraded to supported nickel catalysts (Ni/CAC and Ni/PAC) and applied in methane dry reforming reaction. Ni/CAC showed higher CH_4 conversion (43 %), while Ni/PAC was more suitable for CO_2 conversion (31 %). Our results demonstrate that both CAC and PAC produced by microwave vacuum pyrolysis of PKS show promise for use as catalyst support material.

Acknowledgements The authors gratefully acknowledge financial support from the Universiti Malaysia Terengganu to conduct this research. The authors also thank all the laboratory assistants in Universiti Malaysia Terengganu involved throughout this research for technical support.

References

1. P. Atkins, T. Overton, J. Rourke, M. Weller, *Inorganic Chemistry* (Oxford University Press, New York, 2006)
2. O. Deutschmann, H. Knözinger, K. Kochloefl, T. Turek, *Ullmann's Encyclopedia of Industrial Chemistry* (Wiley, Weinheim, 2009)
3. H.A. Choudhury, V.S. Moholkar, Int. J. Innov. Res. Sci. Eng. Technol. **2**, 8 (2013)
4. N.M. Julkapli, S. Bagheri, Int. J. Hydrogen Energy **40**, 2 (2015)
5. S.S. Lam, R.K. Liew, Y.M. Wong, E. Azwar, A. Jusoh, R. Wahi, Waste Biomass Valoriz. **8**, 2109 (2017)
6. N.T. Phan, D.H. Brown, P. Styring, Tetrahedron Lett. **45**, 42 (2004)
7. E. Antolini, Renew. Sustain. Energy Rev. **58**, 34 (2016)
8. T. Dong, D. Gao, C. Miao, X. Yu, C. Degan, M. Garcia-Pérez, B. Rasco, S.S. Sablani, S. Chen, Energy Convers. Manag. **105**, 1389 (2015)
9. J.R. Kastner, S. Mani, A. Juneja, Fuel Process. Technol. **130**, 31 (2015)
10. S.S. Lam, R.K. Liew, C.K. Cheng, H.A. Chase, Appl. Catal. B Environ. **176**, 601 (2015)
11. B. Wu, Y. Kuang, X. Zhang, J. Chen, Nano Today **6**, 1 (2011)
12. X. Ji, K.T. Lee, R. Holden, L. Zhang, J. Zhang, G.A. Botton, M. Couillard, L.F. Nazar, Nat. Chem. **2**, 4 (2010)
13. B. Meryemoglu, S. Irmak, A. Hasanoglu, Fuel Process. Technol. **151**, 59 (2016)
14. M. Dhelipan, A. Arunchander, A. Sahu, D. Kalpana, J. Saudi Chem. Soc. **21**, 4 (2017)
15. S.S. Lam, R.K. Liew, Y.M. Wong, N.Y.P. Yek, N.L. Ma, C.L. Lee H.A. Chase, J. Clean. Prod. **162**, 1376 (2017)
16. E. Lam, J.H. Luong, ACS Catal. **4**, 10 (2014)
17. N.S. Nasri, M. Jibril, M.A.A. Zaini, R. Mohsin, H.U. Dadum, A.M. Musa, Jurnal Teknologi **67**, 4 (2014)
18. S.S. Lam, R.K. Liew, A. Jusoh, C.T. Chong, F.N. Ani, H.A. Chase, Renew. Sustain. Energy Rev. **53**, 741 (2016)
19. S.S. Lam, R.K. Liew, X.Y. Lim, F.N. Ani, A. Jusoh, Int. Biodeterior. Biodegad. **113**, 325 (2016)
20. G. Li, W. Zhu, L. Zhu, X. Chai, Korean J. Chem. Eng. **33**, 2215 (2016)
21. S.H. Park, H.J. Cho, C. Ryu, Y.-K. Park, J. Ind. Eng. Chem. **36**, 314 (2016)
22. J.S. Cha, S.H. Park, S.-C. Jung, C. Ryu, J.-K. Jeon, M.-C. Shin, Y.-K. Park, J. Ind. Eng. Chem. **40**, 1 (2016)
23. A.R. Mohamed, M. Mohammadi, G.N. Darzi, Renew. Sustain. Energy Rev. **14**, 6 (2010)
24. Y.-J. Zhang, Z.-J. Xing, Z.-K. Duan, M. Li, Y. Wang, Appl. Surf. Sci. **315**, 279 (2014)
25. D.-W. Cho, S.-H. Cho, H. Song, E.E. Kwon, Bioresour. Technol. **189**, 1 (2015)

26. X.-F. Tan, S.-B. Liu, Y.-G. Liu, Y.-L. Gu, G.-M. Zeng, X.-J. Hu, X. Wang, S.-H. Liu, L.-H. Jiang, Bioresour. Technol. **227**, 359 (2017)
27. N.A. Rashidi, S. Yusup, Chem. Eng. J. **314**, 277 (2016)
28. M. Shamsuddin, N. Yusoff, M. Sulaiman, Procedia Chem. **19**, 558 (2016)
29. S.S. Lam, R.K. Liew, C.K. Cheng, N. Rasit, C.K. Ooi, N.L. Ma, J.-H. Ng, W.H. Lam, C.T. Chong, H.A. Chase, J. Environ. Manag. **213**, 400 (2018)
30. M. Carrier, A. Loppinet-Serani, D. Denux, J.-M. Lasnier, F. Ham-Pichavant, F. Cansell, C. Aymonier, Biomass Bioenergy **35**, 1 (2011)
31. R.K. Liew, W.L. Nam, M.Y. Chong, X.Y. Phang, M.H. Su, P.N.Y. Yek, N.L. Ma, C.K. Cheng, C.T. Chong, S.S. Lam, Process Saf. Environ. Prot. (2017). https://doi.org/10.1016/j.psep.2017.10.005
32. W.L. Nam, X.Y. Phang, M.H. Su, R.K. Liew, N.L. Ma, M.H.N. Rosli, S.S. Lam, Sci. Total Environ. **624**, 9 (2018)
33. G. Sethia, A. Sayari, Carbon **99**, 289 (2016)
34. B.V. Ayodele, M.R. Khan, S.S. Lam, C.K. Cheng, Int. J. Hydrogen Energy **41**, 8 (2016)
35. O.U. Osazuwa, C.K. Cheng, J. Clean. Prod. **148**, 202 (2017)
36. T. Srimachai, V. Thonglimp, O. Sompong, Energy Procedia **52**, 352 (2014)
37. S. Ang, E. Shaza, Y. Adibah, A. Suraini, M. Madihah, Process Biochem. **48**, 9 (2013)
38. M.M. Ishola, M.J. Taherzadeh, Bioresour. Technol. **165**, 9 (2014)
39. M. Saidu, A. Yuzir, M.R. Salim, S. Azman, N. Abdullah, Int. Biodeterior. Biodegrad. **95**, 189 (2014)
40. G. Neutelings, Plant Sci. **181**, 4 (2011)
41. J. Cao, G. Xiao, X. Xu, D. Shen, B. Jin, Fuel Process. Technol. **106**, 41 (2013)
42. F.-X. Collard, J. Blin, Renew. Sustain. Energy Rev. **38**, 594 (2014)
43. S.S. Lam, W.A.W. Mahari, C.K. Cheng, R. Omar, C.T. Chong, H.A. Chase, Energy **115**, 791 (2016)
44. S.S. Lam, W.A.W. Mahari, A. Jusoh, C.T. Chong, C.L. Lee, H.A. Chase, J. Clean. Prod. **147**, 263 (2017)
45. W.A. Wan Mahari, N.F. Zainuddin, W.M.N. Wan Nik, C.T. Chong, S.S. Lam, Energies **9**, 780 (2016)
46. W.A. Wan Mahari, N.F. Zainuddin, C.T. Chong, C.L. Lee, W.H. Lam, S.C. Poh, S.S. Lam, J. Environ. Chem. Eng. **5**, 5836 (2017)
47. Y. Shen, P. Zhao, Q. Shao, D. Ma, F. Takahashi, K. Yoshikawa, Appl. Catal. B Environ. **152–153**, 140 (2014)
48. M. Musa, M. Sanagi, H. Nur, W. Ibrahim, Sains Malays. **44**, 4 (2015)
49. K. Sing, D. Everett, R. Haul, L. Moscou, R. Pierotti, J. Rouquerol, T. Siemieniewska, Pure Appl. Chem. **57**, 4 (1985)
50. M.N. Mahamad, M.A.A. Zaini, Z.A. Zakaria, Int. Biodeterior. Biodegrad. **102**, 274 (2015)
51. C. Fukuhara, R. Hyodo, K. Yamamoto, K. Masuda, R. Watanabe, Appl. Catal. A Gen. **468**, 18 (2013)
52. I. Bodrov, L. Apel'baum, Kinet. Catal. **8**, 379 (1967)